JOURNAL OF TISSUE ENGINEERING AND REGENERATIVE MEDICINE
J Tissue Eng Regen Med 2017; **11**: 2116–2126.
Published online 27 November 2015 in Wiley Online Library (wileyonlinelibrary.com) **DOI:** 10.1002/term.2109

RESEARCH ARTICLE

Conditioned media from hypoxic-cultured human dental pulp cells promotes bone healing during distraction osteogenesis

Masahito Fujio[1,2*], Zhe Xing[1], Niyaz Sharabi[1], Ying Xue[1], Akihito Yamamoto[2], Hideharu Hibi[2], Minoru Ueda[2], Inge Fristad[1] and Kamal Mustafa[1*]
[1]*Department of Clinical Dentistry, Centre for Clinical Dental Research, University of Bergen, Norway*
[2]*Department of Oral and Maxillofacial Surgery, Nagoya University Graduate School of Medicine, Japan*

Abstract

Distraction osteogenesis (DO) is a surgical procedure used to correct various skeletal disorders. Improving the technique by reducing the healing time would be of clinical relevance. The aim of this study was to determine the angiogenic and regenerative potential of conditioned media (CMs) collected from human dental pulp cells (hDPCs) grown under different culture conditions. CM collected from cells under hypoxia was used to improve bone healing and the DO procedure *in vivo*. The angiogenic potentials of CMs collected from hDPCs grown under normoxic (−Nor) and hypoxic (−Hyp) conditions were evaluated by quantitative PCR (*VEGF-A*, angiopoietin-1, angiopoietin-2, interleukin-6 (*IL-6*) and *CXCL12*), ELISA assays (VEGF-A, Ang-2), tube-formation and wound-healing assays, using human umbilical vein endothelial cells. The results demonstrated that hypoxic CM had significantly higher angiogenic potential than normoxic CM. Human fetal osteoblasts (hFOBs) were exposed to CM, followed by alizarin red staining, to assess the osteogenic potential. It was found that CM did not enhance the mineralization capacity of hFOBs. DO was performed in the tibiae of 30 mice, followed by a local injection of 20 µl CM (CM–Nor and CM–Hyp groups) or serum-free DMEM (control group) into the distraction zone every second day. The mice were sacrificed at days 13 and 27. The CM–Hyp treatment revealed a higher X-ray density than the control group ($p < 0.05$). Our study suggests that the angiogenic effect promoted by hypoxic culture conditions is dependent on VEGF-A and Ang-2 released from hDPCs. Furthermore, CM–Hyp treatment may thus improve the DO procedure, accelerating bone healing. © 2015 The Authors. *Journal of Tissue Engineering and Regenerative Medicine* published by John Wiley & Sons, Ltd.

Received 5 November 2014; Revised 7 October 2015; Accepted 15 October 2015

Keywords **distraction osteogenesis; conditioned media; regeneration; bone; angiogenesis**

1. Introduction

Distraction osteogenesis (DO) is a surgical procedure to correct a variety of skeletal disorders, such as limb length discrepancies, bone defects, limb deformities and for the reunion of fractures in various congenital and post-traumatic conditions (Watson, 2006). The DO model consists of three phases: the latency phase, after osteotomy and placement of the external distractor; the distraction phase, in which the separated bone ends are gradually and continuously distracted; and the consolidation phase (Ilizarov, 1989). Serial DO treatment allows the formation of new hard and soft tissues. Although this technique is useful in the treatment of orthopaedic disorders, the main disadvantages are the considerable time required to lengthen the bone and the use of distraction devices for extended periods (Abbaspour *et al*., 2009). Therefore, improving the DO technique by reducing the healing period would be of clinical importance.

Stem cell therapy has been shown to have beneficial effects on bone tissue regeneration (Yamada *et al*., 2004). Promising results have been reported in both animals

**Correspondence to:* Masahito Fujio and Kamal Mustafa, Department of Clinical Dentistry, Centre for Clinical Dental Research, University of Bergen Årstadsv. 19 5009, Bergen, Norway. E-mail: m-fujio@med.nagoya-u.ac.jp; kamal.mustafa@iko.uib.no

and humans, although the level of engraftment and differentiation of the cells could be improved (Ide *et al*., 2010; Toma *et al*., 2002). Recently, the role played by paracrine factors produced by stem cells in tissue regeneration and healing has been investigated and reports have demonstrated that angiogenesis and osteogenesis are promoted by conditioned medium (CM) collected from bone marrow mesenchymal stem cells (BMMSCs) (Chen *et al*., 2008; Osugi *et al*., 2012).

It is well known that primitive stimuli, such as hypoxic conditions and mechanical stress, can change the characteristics of cells and the factors they secrete (Wang and Thampatty, 2006; Wang *et al*., 2007). For example, the hypoxia-inducible factor (HIF-1) pathway senses changes in local oxygen availability and responds via transcriptional activation of two pro-angiogenic factors, vascular endothelial growth factor (VEGF)-A and angiopoietins (Ang). Mechanical stress is also known to be a stimulus that influences bone metabolism, with demonstration that bone tissue and osteoprecursor cells respond to mechanical stress both *in vitro* and *in vivo* (Rubin *et al*., 2006).

Dental pulp stem cells, which can be collected from dental pulp, have phenotypic characteristics similar to those of BMMSCs (Shi *et al*., 2001). These cells can differentiate into the dentinogenic lineage, the mesodermal lineage or the ectodermal lineage cell (Egusa *et al*., 2012) and secrete various cytokines and chemokines (Aranha *et al*., 2010; Gong *et al*., 2010). Moreover, these cells can be collected without adverse health problems. Thus, these previous reports support the use of dental pulp cells as a unique cellular resource for regeneration therapies. However, their possibilities for bone regeneration in DO is mostly unknown. *In vitro* experiments were performed, aiming to determine the angiogenic and regenerative potential of conditioned media (CMs) collected from human dental pulp cells grown under normoxic and hypoxic culture conditions. Furthermore, CMs collected from cells cultured under hypoxia were used to accelerate bone healing and improve the DO surgical procedure *in vivo*.

2. Materials and methods

The overall experimental design is summarized in Figure 1A–C.

2.1. Isolation of hDPC and cell culture

hDPCs were isolated as previously described (Gronthos *et al*., 2000). Briefly, adult third molars or premolars (from patients aged 18–25 years) scheduled for extraction were collected (six teeth in total). Informed consent was obtained from each patient, and the Ethical Committee at the University of Bergen, Norway, approved the research protocol. After separation of the crowns from the roots, dental pulps were isolated and then digested in a solution of 3 mg/ml collagenase type I and 4 mg/ml dispase for 1 h at 37 °C. Single-cell suspensions (1×10^4–2×10^4 cells/ml) were plated on culture dishes in Dulbecco's modified Eagle's medium (DMEM; PAA, GE

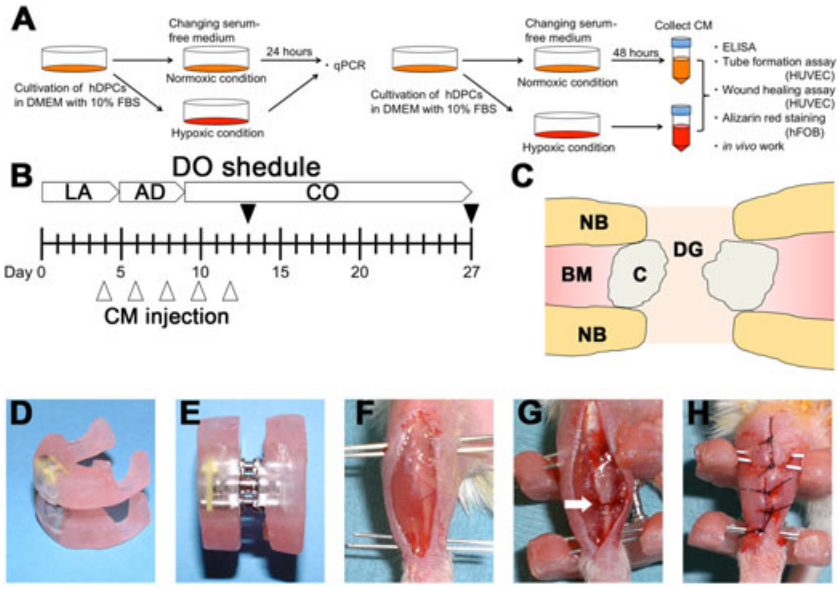

Figure 1. Outline of the study: (A) *in vitro* experiments and analyses; (B) *in vivo* distraction schedule and experimental design; after a 5 day latency period, distraction was started at a rate of 0.4 mm/12 h and continued for 4 days, increasing the length of the bone defect by 3.2 mm: black arrowheads, time points of sacrifice; white arrowheads, time points for injecting 20 µl of either control medium (control), CM–Nor or CM–Hyp; LA, latency period; AD, active distraction period; CO, consolidation period. (C) Schematic drawing of distraction site: NB, native bone; BM, bone marrow; C, callus; DG, distraction gap. (D–H) A custom-made distractor was composed of two incomplete acrylic resin rings and an expansion screw: an anterior longitudinal incision was made on the right lower limb of each mouse; needles were inserted through the skin into the proximal and distal metaphysis of the tibia; subsequently, sets of needles were fixed to the custom-made fixator with acrylic resin; after polymerization of the resin, osteotomy was carried out at the middle of the diaphysis (white arrow); the wound was closed with a 4–0 nylon suture. [Colour figure can be viewed at wileyonlinelibrary.com]

DOI: 10.1002/term

Healthcare, Little Chalfont, UK) supplemented with 10% fetal calf serum (FCS) and 1% antibiotic mixture comprising penicillin–streptomycin, before incubation at 37 °C in 5% CO_2. Cells at passages 4–8 were used for all experiments.

2.2. CM preparation

When the hDPCs reached 80% confluence, the media were replaced with serum-free DMEM containing penicillin–streptomycin and cultured for 48 h at 37 °C in an atmosphere of 21% O_2 and 5% CO_2 (normoxic cells) or in a hypoxic chamber (Stem Cell Technology, Vancouver, BC, Canada) containing 1% O_2 and 5% CO_2, (hypoxic cells). Then the CMs were collected and centrifuged for 5 min at room temperature. The collected CMs were defined as CM–Nor and CM–Hyp, respectively. The collected CMs were stored at 4 °C before being used for the following experiments.

2.3. RNA expression assay in hDPC

Cells at passages 4–6 were plated at a density of 5.0×10^5 in 10 cm culture dishes (Nunc, Roskilde, Denmark). After the cells had reached 80% confluence, they were exposed to normoxic or hypoxic conditions for 24 h. The total RNA collected from hDPCs was extracted using a Maxwell® 16 LEV Simply RNA Cells Kit and a Maxwell® 16 Instrument (Promega, Fitchburg, WI, USA), according to the manufacturer's instructions. RNA purity and quantification were determined by spectrophotometry (Nanodrop Spectrophotometer, ThermoScientific NanoDrop Technologies, Wilmington, DE, USA). First-strand cDNA synthesis was carried out using a High-Capacity cDNA Archive Kit (Applied Biosystems, Carlsbad, CA, USA) from 1 μg total RNA.

Quantitative real-time transcription–polymerase chain reaction (qPCR) was performed in StepOne Plus (Applied Biosystems), with fast enzyme and cycling conditions, on a StepOne real-time PCR system, using TaqMan® gene expression assays (Applied Biosystems). Data of these targeted genes were normalized to the internal control glyceraldehyde-3-phosphate dehydrogenase (*GAPDH*) to obtain ΔC_T. The final quantities of the genes of interest, relative to those seen in samples from normoxic cells, were reported by $2^{-\Delta\Delta C_T}$ method. Primer sets are listed in Table 1.

2.4. CM and angiogenic growth factor expression

The levels of VEGF-A and Ang-2 in CMs collected from hDPCs grown under normoxic or hypoxic conditions for 48 h were investigated using enzyme-linked immunosorbent assay (ELISA). The concentration of these growth factors was measured using a Human Quantikine ELISA Kit (DVE00 and DANG20, R&D Systems, Minneapolis, MN, USA), according to the manufacturer's instructions.

Table 1. Primer Accession Nos used in qPCR

Species	Gene	Taqman assay ID
Human	*GAPDH*	Hs02758991_g1
Human	*VEGFA*	Hs00900055_m1
Human	*ANG-1*	Hs00375822_m1
Human	*ANG-2*	Hs01048042_m1
Human	*IL-6*	Hs00985639_m1
Human	*CXCL12*	Hs03676656_mH
Mouse	*β-Actin*	Mm00607939_s1
Mouse	*Runx2*	Mm00501584_m1
Mouse	*Sp7*	Mm04209856_m1
Mouse	*Sox5*	Mm01264584_m1
Mouse	*Sox9*	Mm00448840_m1
Mouse	*F8*	Mm01215675_m1

GAPDH, glyceraldehyde-3-phosphate dehydrogenase; *VEGFA*, vascular endothelial growth factor-A; *ANG-1*, angiopoietin-1; *ANG-2*, angiopoietin-2; *IL-6*, interleukin-6; *CXCL12*, C–X–C motif chemokine 12; *Runx2*, runt-related transcription factor 2; *Sp7*, Osterix; *F8*, factor 8

2.5. Tube formation assay

Passage 2–3 human umbilical vein endothelial cells (HUVECs; C2517A; Lonza, Walkersville, MD, USA) at 80% confluence were suspended in CM–Nor or CM–Hyp and cultured at a density of 1.0×10^5, in duplicate, in 96-well plates coated with Growth Factor Reduced Matrigel (356230, BD Biosciences, San Jose, CA, USA). EGM-2 BulletKit (CC-3162, Lonza) and serum-free DMEM were used as positive and negative controls, respectively. After 8 h, the formation of tube-like structures was examined using a microscope. Photographs were taken and the number of branch points, total tube lengths and tube formation areas (see supporting information, Figure S1A) were measured and assayed, using the NIS-Elements software program BR 3.07 (Nikon, Tokyo, Japan).

2.6. Endothelial cell wound-healing assay

Passage 2–3 HUVECs were cultured in Culture-Insert 24 (80241, Ibidi, Martinsried, Planegg, Germany) at a concentration of 3.0×10^4 cells/well, in duplicate. After the cells had reached 80% confluence, the culture inserts were gently removed using sterile tweezers. The wounded monolayers were then washed three times with phosphate-buffered saline (PBS) to remove cell debris and incubated with normoxic and hypoxic CMs and positive/negative control media. After 24 h of incubation, the cells were fixed and stained with crystal violet. The area of cell-free wound was recorded using a microscope. Photographs were taken of each well, measured and assayed using Photoshop CS5 (Adobe Systems, San Jose, CA, USA) and the ImageJ software program v. 1.43 (NIH, Bethesda, MD, USA). The wound-healing effect was calculated as the percentage of the remaining cell-free area compared with the area of the initial wound.

DOI: 10.1002/term

2.7. Alizarin red staining

Human fetal osteoblasts (hFOBs; CRL-11372, ATCC, Manassas, VA, USA) were cultured in 24-well plates at a concentration of 5.0×10^4 cells/well, with DMEM supplemented with 10% FBS at 34 °C in an atmosphere containing 21% O_2 and 5% CO_2. When the cells had reached 80% confluence, the media were replaced with DMEM, normoxic or hypoxic CM, all media supplemented with 1% FBS. After 14 days of culture, the cells were stained with a saturated solution of alizarin red S adjusted to pH 4.2 (A5533, Sigma-Aldrich, St. Louis, MI, USA).

2.8. Mouse DO model

All animal experiments were performed in accordance with the Guidelines for Animal Experiments at the University of Bergen. Thirty 8–10 week-old female NMRI mice were used. The surgical DO method was performed as previously described (Fujio *et al*., 2011; Isefuku *et al*., 2000). The fixator was composed of two incomplete acrylic resin rings (outer diameter 20 mm, inner diameter 10 mm, thickness 5 mm) and an expansion screw (600-301-30, Ortho Dentaurum, Berlin, Germany) (Figure 1D, E). The total weight of the device, including the needles inserted into the tibia, was 2.7 g. The animals were anaesthetized by isoflurane (Isoba Vet, Schering-Plough, Lysaker, Norway). The right limb was carefully shaved and disinfected with 10% iodine solution. A longitudinal skin incision was made on the right leg and the underlying muscles were bluntly separated, taking care not to remove all of the periosteum. The fibula was fractured by direct lateral pressure. The tibia was fixed to the device with one pair of 25 gauge needles proximally and one pair of 27 gauge needles distally, glued with acrylic resin (Figure 1F). After complete polymerization (ca. 5 min), an osteotomy was performed at the middle of the diaphysis (Figure 1G). This was done using very small cutting forceps. The wound was closed with a 4–0 nylon suture (Figure 1H).

After a latency period of 5 days, distraction was started at a rate of 0.4 mm/12 h. The lengthening was continued for 4 days, resulting in a gap of 3.2 mm in total; 20 µl CM or serum-free DMEM as control were injected transcutaneously into the centre of the distraction gap every second day during days 4–12 after operation (five injections in total), using a syringe (Hamilton, Bonaduz, Switzerland) (Figure 1C). We defined the following groups, based on the injection protocol: control group ($n = 5$); CM–Nor ($n = 5$); CM–Hyp ($n = 5$). The mice were sacrificed at days 13 and 27 after surgery ($n = 5$/group) (Figure 1B).

2.9. Assessment of transcription factors during DO

Tissue collected from the distal distraction gap was excised and stored in liquid nitrogen until RNA extraction at day 13 ($n = 5$). Total RNA was extracted using TRIzol (Invitrogen, Carlsbad, CA, USA). RNA purity and quantification were determined by Nanodrop spectrophotometry. First-strand cDNA synthesis was carried out using the High-Capacity cDNA Archive Kit (Applied Biosystems) from 1 µg total RNA. qPCR was performed in StepOne Plus (Applied Biosystems), with fast enzyme and cycling conditions, on a StepOne real-time PCR system, using TaqMan® gene expression assays (Applied Biosystems). Data of these targeted genes were normalized to the internal control β-actin to obtain ΔC_T. The final quantities of the genes of interest, relative to control samples, were reported by the $2^{-\Delta\Delta C_T}$ method. Primer sets are listed in Table 1.

2.10. Radiographic and histological analysis

Digital X-ray images were taken at days 13 and 27 after surgery, using a Kodak Multispectral FX instrument (Carestream Health, Toronto, Canada). The distraction gap was outlined from the outside corners of the two proximal and the two distal cortices, forming a quadrilateral region of interest (ROI). The X-ray density of newly formed bone was analysed using Bruker MI SE software, v. 7.1.3 (Scrum, Osaka, Japan). After the animals had been sacrificed, the distracted tibias were fixed in 10% neutral buffered formalin for 24 h at room temperature. Samples were decalcified with Morse's solution (10% sodium citrate, 20% formic acid) overnight at 4 °C. The samples were then washed in PBS and embedded with OCT™ (Sakura Finetek, Tokyo, Japan), after which 8 µm sections were made on a cryostat (Leica CM 3050S, Leica Microsystems, Wetzlar, Germany). The cryosections were stained with haematoxylin and eosin (H&E) and safranin O–fast green. In the sections of each sample, the percentage area of newly formed cartilage and bone was measured. The pixel number of each area in the distraction zone was counted using Image J, v. 1.43 (NIH, Bethesda, MD, USA) (see supporting information, Figure S1B).

2.11. Immunohistochemistry

The sections were washed in PBS, blocked with 1% bovine serum albumin (BSA)/PBS for 30 min and then incubated with the primary antibody [rabbit polyclonal antibody (Ab) α-SMA; ab5694, Abcam, Cambridge, UK) in blocking buffer for 1 h. The sections were then incubated with the secondary antibody, conjugated with AlexaFluor 555 (Life Technologies, Waltham, MA, USA) for 30 min. The cell nuclei were labelled with diamidinophenylidole (D1306; Life Technologies). The sections were finally mounted with Prolong Gold Antifade Reagent (P36934, Life Technologies). Vascular density was assessed morphometrically by examining five fields/section of the distraction gap, in three successive sections, after immunofluorescence staining using the anti-α-SMA Ab. Images were

DOI: 10.1002/term

captured using an Eclipse 80i fluorescence microscope (Nikon, Tokyo, Japan).

2.12. Statistical analysis

Statistical analysis was performed using the SPSS statistical package v. 19.0 (IBM, Armonk, New York, USA). Paired Student's *t*-test was used for comparisons. One-way analysis of variance (ANOVA) was applied to compare two or more means, followed by the Tukey HSD test. The results were expressed as mean ± standard deviation (SD); $p < 0.05$ was considered statistically significant.

3. Results

3.1. Effect of hypoxia on the angiogenic properties of CMs from hDPCs *in vitro*

Results obtained from qPCR (Figure 2A) and ELISA (Figure 2B, C) showed that *VEGF-A* and *Ang-2* were upregulated in hDPCs grown under hypoxic conditions. The mRNA expressions of *VEGF-A* and *Ang-2* were approximately two- and 1.5-fold higher, respectively, when compared with their expression under normoxic conditions ($p < 0.05$). On the other hand, *Ang-1* and *CXCL12* expressions were three- to four-fold lower under hypoxic than under normoxic conditions ($p < 0.01$). *IL-6* expression was not significantly different under hypoxic and normoxic conditions (Figure 2A). ELISA was performed to confirm the qPCR results at the protein level. Both VEGF-A165 and Ang-2 protein expression increased significantly under hypoxic conditions ($p < 0.05$) compared with the normoxic group (Figure 2B, C).

3.2. Effect of CM from hDPC on angiogenesis and mineralization *in vitro*

To evaluate the angiogenic activity of CM, we performed both the Matrigel tube formation assay and the endothelial cell wound-healing assay, using HUVECs. In the control group, HUVECs demonstrated little tube formation (Figure 3A). In contrast, the CM group demonstrated increased endothelial tube formation (Figure 3B, C). The numbers of branch points, total tube lengths and tube formation areas were significantly greater in the hypoxic than in the normoxic and control groups (Figure 3D–F). To further evaluate the angiogenic properties of CM, we performed an endothelial cell wound-healing assay using HUVECs. Hypoxic conditions significantly accelerated wound closure compared to the control and normoxic group (Figure 4A–D). To assess the mineralization capacity of CM, we performed alizarin red staining with hFOBs, which have a high mineralization capacity. hFOBs produced mineral deposits when cultured in DMEM supplemented with 10% FBS (Figure 5A). Mineral deposition was decreased by low serum concentrations (Figure 5B). CM–Nor and CM–Hyp did not enhance the mineralization capacity of hFOBs (Figure 5C, D).

3.3. Effect of CM on DO healing in mouse tibiae

Histological evaluation of the distraction sites showed less newly formed callus and cartilage in the control group than in the CM groups at day 13 (Figure 6A–F). The centre of the distraction site of the control group was filled with fibrous tissue. In contrast, the hypoxic CM group showed massive callus formation at the centre of the distraction site and some cartilage formation in the periosteal region. Interestingly, the normoxic CM group showed greater cartilage formation at the periosteal and distraction sites. To further investigate the role of CM, we performed qPCR assays on day 13 samples (Figure 6G). Osteoblastic and chondrogenic markers were consistent with the histology seen, with the animals exposed to hypoxic CM showing twice as much Osterix expression as the control group ($p < 0.05$). However, there was no significant difference seen for osteoblastic and chondrogenic markers between the normoxic and hypoxic CM groups, which showed approximately 2.5- and two-fold higher Sox 5 expression, respectively, than the control group. Only the normoxic group was significantly different from the control group ($p < 0.05$). Significantly upregulated Factor 8 gene was observed in the hypoxic group

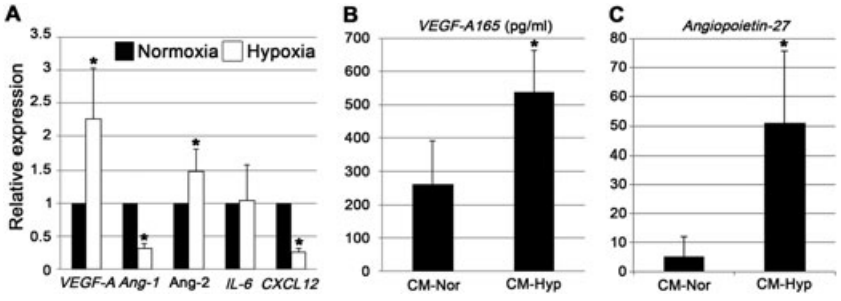

Figure 2. Expression of angiogenic factors from hDPCs under normoxic and hypoxic culture conditions. (A) qPCR assay of mRNA extracted from hDPCs 24 h after normoxic and hypoxic incubation conditions ($n = 6$); *VEGF-A* and *Ang-2* were both upregulated under hypoxic culture conditions. (B, C) CMs were collected after incubation under nomoxic and hypoxic conditions for 48 h ($n = 6$); *VEGF-A 165* (B) and *Ang-2* (C) were both upregulated under hypoxic culture conditions. Data represent mean ± SD; *$p < 0.05$

DOI: 10.1002/term

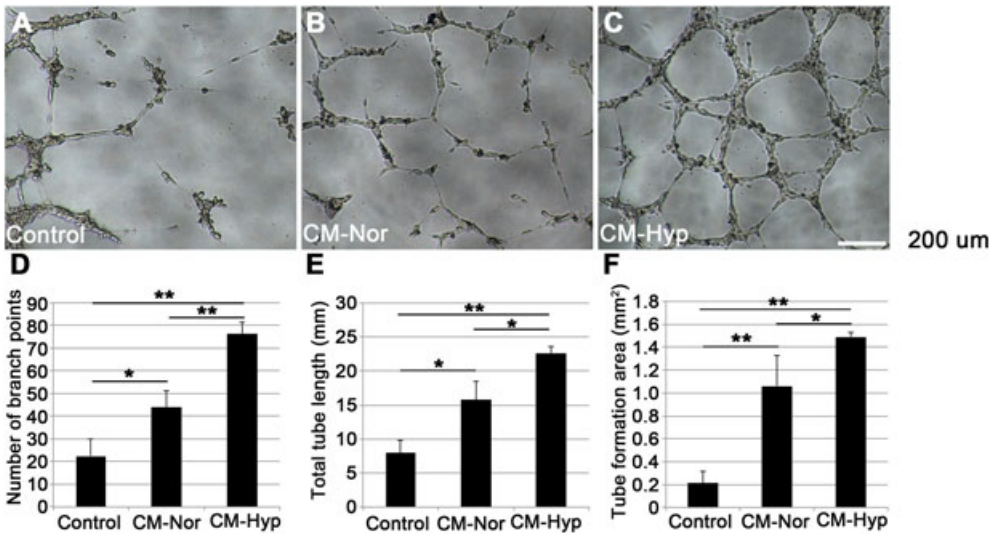

Figure 3. CMs from hDPCs enhance endothelial cell tube formation *in vitro*. The angiogenic potentials of CMs were tested by Matrigel tube formation assay ($n = 6$); HUVECs were suspended in CM–Nor or CM–Hyp in duplicate; tube formation was also observed after culture in serum-free DMEM and EGM-2 Bullet Kit as negative and positive controls (data not shown), respectively; photographs are from (A) control, (B) CM–Nor and (C) CM–Hyp cultures. Number of branch points (D), total tube length (E) and tube formation area (F) were calculated using NIS elements software: the CM–Nor cultures showed higher tube formation than the control cultures; the CM–Hyp cultures showed greater angiogenic potential than CM–Nor cultures; data represent mean ± SD; $^{**}p < 0.01$, $^{*}p < 0.05$; bar = 200 μm. [Colour figure can be viewed at wileyonlinelibrary.com]

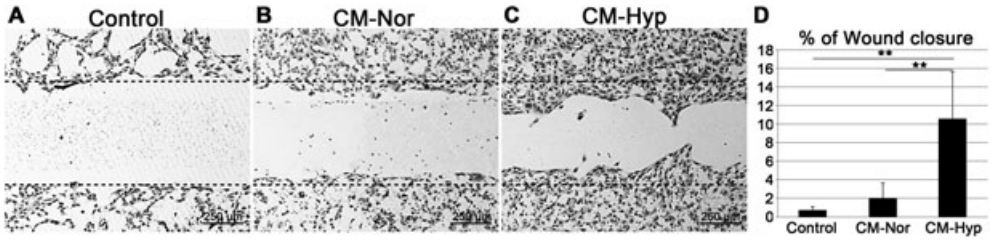

Figure 4. CM from hypoxic conditions promotes endothelial cell migration *in vitro*. Wound-healing assays were performed to assess the angiogenic potentials of CMs from hDPCs. HUVECs were cultured in Culture-Insert 24-well plates, in duplicate; after the cells had reached 80% confluence, the Culture-Insert was gently removed; the wounded monolayers were incubated with CM–Nor (B) and CM–Hyp (C) and both positive (data not shown) and negative (A) control media. After 24 h of incubation, the cells were fixed and stained with crystal violet; the percentage of wound closure was calculated using ImageJ software. (D) CM–Hyp cultures showed greater angiogenic potential compared with the others; data represent mean ± SD; $^{**}p < 0.01$; bar = 250 μm; line of black dots represents base line

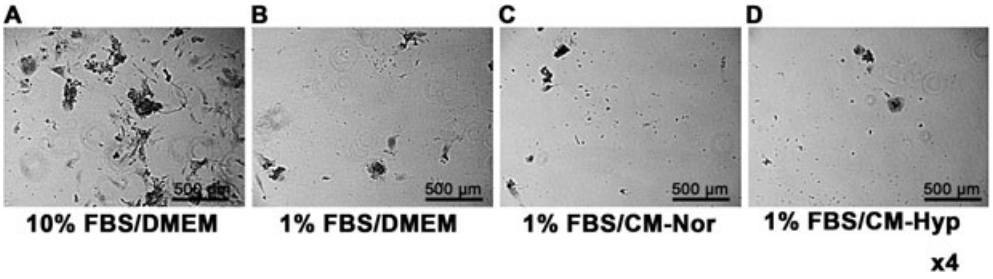

Figure 5. Effect of CM on the mineralization capacity of hFOBs: these were cultured with (A) DMEM supplemented with 10% FBS; (B) DMEM supplemented with 1% FBS; (C) CM–Nor supplemented with 1% FBS; and (D) CM–Hyp supplemented with 1% FBS; bar = 500 μm

compared to the control ($p < 0.01$) and normoxic ($p < 0.05$) groups. Histological and qPCR findings were confirmed by immunohistochemistry. Injection of CM increased α-SMA-positive mature blood vessels at the site of distraction. Furthermore, the hypoxic CMs showed increased blood vessel formation compared with the normoxic group ($p < 0.01$) (Figure 7A–D).

To evaluate DO healing, newly formed bone was assessed radiologically on days 13 and 27. On day 13 there was little bone formation in any of the groups

DOI: 10.1002/term

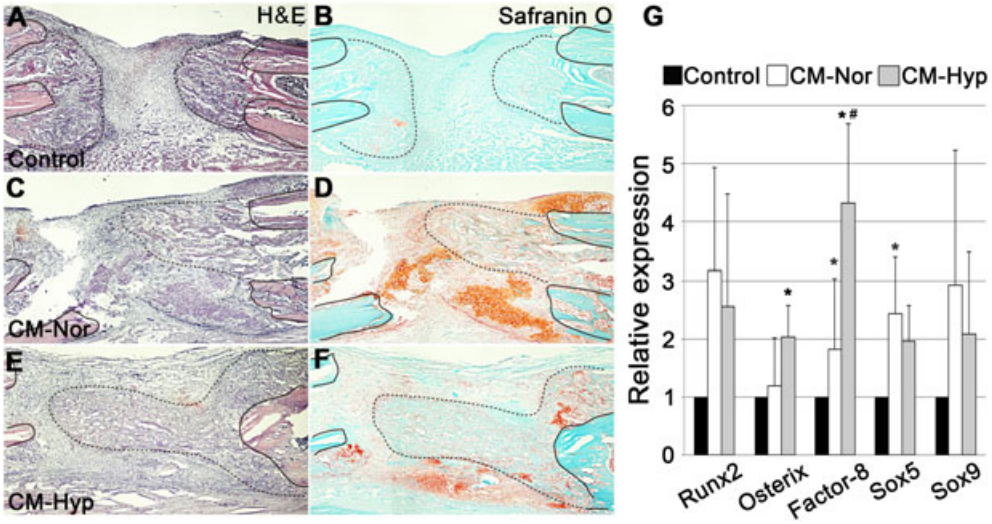

Figure 6. Local administration of CM–Hyp promotes new callus formation in the DO gap: representative micrographs of sections displaying the DO gap stained with H&E (A, C, E) and safranin O–fast green (B, D, F); $n = 5$. Black line on each figure indicates the end of the distal (left side) and proximal (right side) bone fragment; line of black dots on each figure shows newly formed callus: neocallus formation and much fibrous tissue were evident within the DO gap in the control group at day 13 (A, B); little cartilage was observed in the control group (B); the DO gap in the CM–Hyp group showed well generated newly formed callus and periosteum-derived cartilage (E, F); the gap in the CM–Nor group showed massive cartilage and a little callus formation (C, D). To evaluate the effect of the CM on mRNA, DO gap tissue was taken from each group at day 13 ($n = 5$); qPCR results showed significant differences between exposure to CM–Nor and CM–Hyp in Factor 8 gene mRNA (G). Data represent mean ± SD; $^{*}p < 0.05$ vs control, $^{\#}p < 0.05$ vs CM–Nor; bar = 250 μm. [Colour figure can be viewed at wileyonlinelibrary.com]

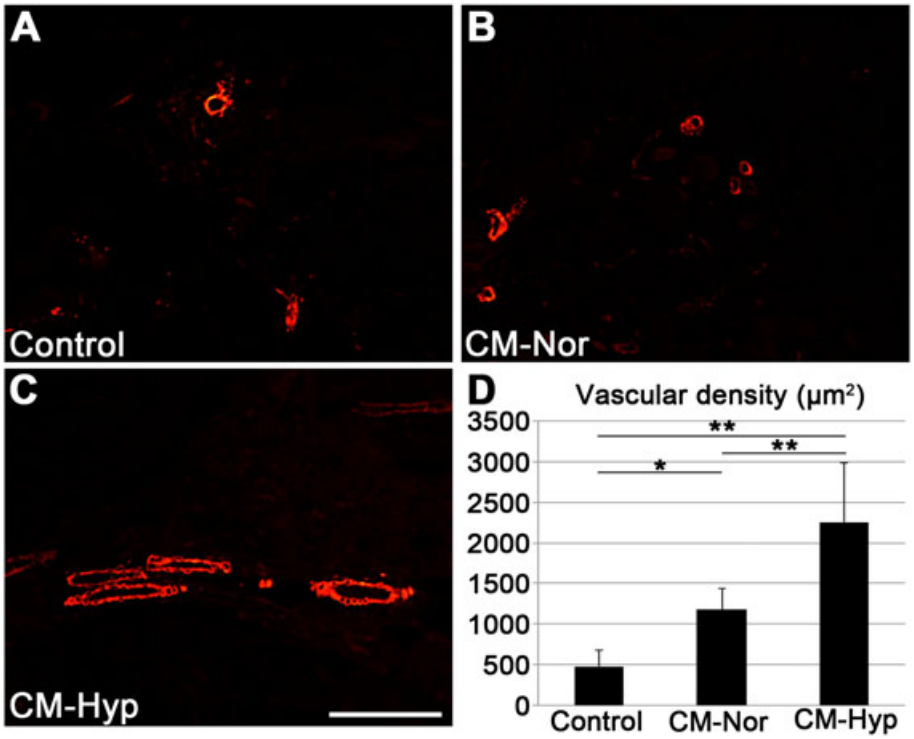

Figure 7. Injection of CM promotes mature blood vessel regeneration. Blood vessel regeneration was assessed by immunofluorescence staining for α-SMA ($n = 5$). Both CM–Nor (B) and CM–Hyp (C) showed significantly higher vascular density (D) compared with control (A); moreover, CM–Hyp showed greater blood vessel regeneration than CM–Nor. Data represent mean ± SD; $^{**}p < 0.01$, $^{*}p < 0.05$; bar = 100 μm. [Colour figure can be viewed at wileyonlinelibrary.com]

(Figure 8A, C, E). On day 27 the control group showed weakly calcified and narrow newly formed bone at the distraction site (Figure 8B, D, F). In contrast, the hypoxic CM group revealed strongly calcified bone at the distraction site (Figure 8F). In addition, the X-ray density of the DO gap was higher in this group than in the control group (Figure 8G, $p < 0.05$). Histological findings also revealed that the CM–Hyp group showed a significantly higher bone formation area compared with the control group at day 27 (Figure 9A–C, G). There was no

DOI: 10.1002/term

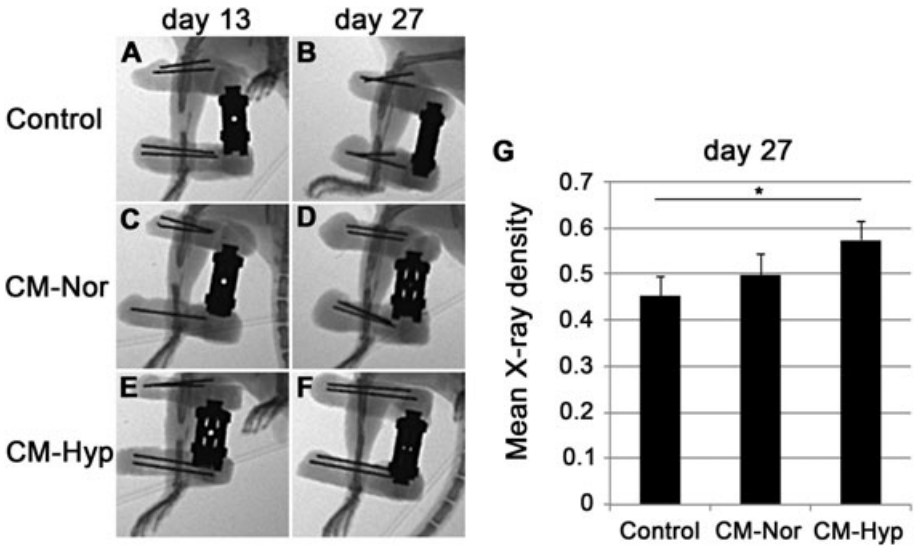

Figure 8. CM from hypoxia promotes healing during DO: newly formed bone was assessed radiologically on days 13 (A, C, E) and 27 (B, D, F) ($n = 5$). There was no significant difference between CMs on day 13; on day 27 the controls (B) showed some calcified and narrow bone formation in the distraction site; the CM–Nor group showed calcified bone formation in the DO gap (D); the CM–Hyp group (F) had strongly calcified bone formation with high X-ray density in the distraction site compared with controls (G). Data represent mean ± SD; $*p < 0.05$

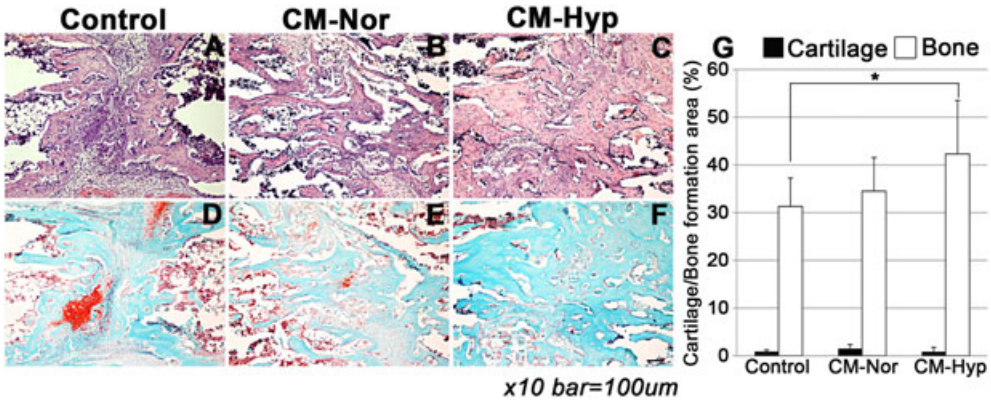

Figure 9. Local administration of CM enhances bone formation: newly formed bone and cartilage were assessed by H&E (A–C) and safranin O–fast green (D, E, F) staining ($n = 5$). The CM–Hyp group showed a significantly higher bone-formation area compared with the control group at day 27 (G); there were no significant differences in the three groups in cartilage formation areas on day 27. Bar = 100 μm; data represent mean ± SD; $*p < 0.05$. [Colour figure can be viewed at wileyonlinelibrary.com]

significant difference between the three groups in the cartilage formation areas at day 27 (Figure 9D–F, G).

4. Discussion

In previous studies, our group has shown that CM from BMMSCs has regenerative potential in several animal bone defect models (Osugi *et al*., 2012; Inukai *et al*., 2013), including DO healing through recruitment of BMMSCs, endothelial cells (ECs) and endothelial progenitor cells (EPCs) (Ando *et al*., 2014). The latter authors focused on monocyte chemoattractant protein (MCP)-1 and MCP-3 in CM from BMMSCs and stated that these chemokines are essential factors in recruiting BMMSCs and ECs/EPCs. In the present study, human dental pulp cells (hDPCs) derived from healthy third molars or premolars extracted during routine surgery were prepared and used according to the protocol described previously (Gronthos *et al*., 2000). Dental pulp is a heterogeneous mixture of various cells, such as ECs, odontoblasts, fibroblasts and mesenchymal stem cells. The 'stemness' of dental pulp cells has been evaluated in several studies (Al-Sharabi *et al*., 2014; Sakai *et al*., 2012). Although these cells have stem cell properties, such as multi-differential and self-renewal capacity comparable to other adult stem cells (Egusa *et al*., 2012), hDPCs have higher proliferative capacity than BMMSCs (Alge *et al*., 2010). Furthermore, hDPCs can be obtained easily from teeth that are scheduled for ordinary extraction, and therefore with fewer ethical considerations. The results obtained from this study suggest that hDPCs have advantages as a cell source for regenerative therapy.

Hung *et al*. (2007) investigated *in vitro* the release of cytokines from BMMSCs grown under normoxic and hypoxic conditions, using cytokine arrays. In their study,

DOI: 10.1002/term

higher expression of angiogenic factors such as VEGF, MCP-1 and angiogenin was found in the CMs collected from cells cultured under hypoxic conditions. Chen *et al*. (2008) also revealed an advantage of hypoxic culture conditions on the secretion of angiogenic factors from BMMSCs.

Accordingly, the *in vitro* and *in vivo* experiments performed in the present study clearly demonstrated profound stimulatory effects of hypoxia on angiogenesis. This indicates that hypoxia may induce the angiogenic properties of stem cell in general.

We evaluated the expression of angiogenic factors derived from hDPCs cultured under hypoxic conditions. It has previously been suggested that the angiogenic potential of hDPCs is enhanced by hypoxic culture conditions (Ceradini *et al*., 2004; Aranha *et al*., 2010). It was demonstrated that hypoxic-cultured hDPCs increased the expression of *HIF-1*, recognized as a master gene of angiogenesis, and *VEGF*, reported to be a major regulator of angiogenesis at the protein level. In this study, we showed that hypoxia induced not only *VEGF* but also *Ang-2* upregulation at both the gene and protein levels. Moreover, we demonstrated the angiogenic potential of hypoxic CMs by using both *in vitro* and *in vivo* models. However, we did not observe *CXCL12* gene upregulation in hDPCs, a result that is consistent with previous findings (Gong *et al*., 2010). The latter authors examined the regulation of the *CXCL12–CXCR4* axis in hDPC cultured under hypoxic conditions and found an increased expression of *HIF-1* and *CXCR4* mRNA, but a decreased expression of *CXCL12* mRNA over a 24 h culture period. We evaluated the expression of *Ang-1*, which has been previously reported as an angiogenic growth factor generating a stable and functional vasculature (Suri *et al*., 1996). In this *in vitro* study, the *Ang-1* level of hDPCs was reduced by hypoxia. Generally, it is known that hypoxia induces *Ang-2* mRNA expression in endothelial cells (Pichiule *et al*., 2004). In contrast, *Ang-1* is reported to be downregulated by hypoxia (Enholm *et al*., 1997). However, Park *et al*. (2003) reported that hypoxia upregulated *Ang-1* mRNA in retinal pericytes. Further studies are needed to elucidate the relationship between hypoxia and angiopoietic agents.

The *in vitro* angiogenic potential of CM was tested by Matrigel tube formation and wound-healing assays, using HUVEC. These assays have been widely used to evaluate angiogenic potential *in vitro* (Ashton *et al*., 1999). In both assays, CM–Hyp had a greater angiogenic effect than control medium and CM–Nor. We examined the mRNA expression of basic fibroblast growth factor, hepatocyte growth factor, epidermal growth factor and chemokine (C–C motif) ligand 2 (data not shown), as these factors have previously been reported to be angiogenic (Bikfalvi *et al*., 1997; Morishita *et al*., 1999; Shen *et al*., 2010; Stamatovic *et al*., 2006). However, the mRNA expression for these growth factors was reduced under hypoxic culture conditions. This suggests that VEGF-A and Ang-2 were the main growth factors responsible for the enhanced *in vitro* angiogenesis found in this study. Previous *in vitro* reports have also suggested that both VEGF-A and Ang-2 are important for angiogenesis (Halin *et al*., 2008; Kim *et al*., 2009). We therefore suggest that these factors enhanced bone formation through blood vessel formation in our DO model. Angiogenesis involves the sprouting and remodelling of the primitive vessels and the subsequent stabilization of the sprouts by α-SMA-positive mural cells (pericytes in medium-sized vessels and smooth muscle cells in larger ones). It is well known that expression of *VEGF-A* and *Ang-2* is observed at sites of vascular remodelling. Moreover, Ang-2 has been shown to have a VEGF-dependent modulation of capillary structure and endothelial cell survival *in vivo* (Lobov *et al*., 2002; Maisonpierre *et al*., 1997). Our study suggests that the angiogenic effect seen *in vivo* is promoted by an increased amount of VEGF-A and Ang-2 in the hypoxic CM. In this study, CM–Hyp did not change the mineralization capacity of hFOBs *in vitro*. Therefore, we suggest that CM–Hyp promotes DO healing through enhanced angiogenesis. Further studies are needed to elucidate the possible osteogenic effects of CM–Hyp *in vivo*.

As bone formation interacts strongly with blood vessel formation (Carano and Filvaroff, 2003; Carmeliet, 2003; Kanczler and Oreffo, 2008), we propose that the effect of conditioned media on DO healing is effected primarily through blood vessel formation. The newly formed blood vessels can transport oxygen, nutrients, soluble growth factors and various types of cells, which collectively play a key role in bone formation. It is also well known that, during DO healing, bone regeneration is induced by blood vessel regeneration (Li, 1999). The qPCR results at day 13 showed no significant difference in the expression of osteogenic and chondrogenic markers between the normoxic and hypoxic groups *in vivo*. However, we observed significantly higher expression of Factor-8, a marker for blood vessel formation. Further, the immunohistochemistry results also showed that the average α-SMA-positive mature vascular density in the hypoxic group was about twice that in the normoxic group. Additional evidence supporting the concept that the bone healing observed in the present study is dependent on angiogenesis comes from the finding that CM did not enhance mineralization *in vitro*. These results suggest that injection of CM enhanced DO healing through the formation of α-SMA-positive blood vessels. A recent report, using a cell-based transplantation approach, showed that the transplantation of stem cells from human dental pulp into the distraction site promoted DO healing (Alkaisi *et al*., 2013). Taken together, our data suggest that the paracrine angiogenic signalling/growth factors derived from dental pulp cells may have a significant role in bone healing.

Although stem cell implantation has beneficial effects on specific diseases, the implanted stem cells cannot survive for a long time (Ide *et al*., 2010; Toma *et al*., 2002). As a consequence, it has been proposed that paracrine factors secreted by the implanted stem cells are of crucial importance for the beneficial effects that are observed after stem cell implantation. Therefore, we tested whether CM from hDPCs contains factors that promote DO healing. Local administration of CM–Hyp

DOI: 10.1002/term

may improve the DO procedure by a reduction in healing time.

In summary, the biological effect of CM from hDPCs can be modified by culture conditions. Hypoxic culture conditions stimulated an upregulation of angiogenic factors secreted from hDPCs. Local administration of CM from hDPCs cultured under hypoxic conditions promoted blood vessels and bone formation in the DO gap. Our results suggest that paracrine factors secreted from hDPCs can be optimized for use in DO treatment by altering the culture conditions.

Conflict of Interest

The authors have declared that there is no conflict of interest.

Acknowledgements

The authors thank Dr Yuji Ando and Ms Siren Østvold for their encouragement to complete this study, which was supported by the University of Bergen and the Meltzer Foundation.

References

Abbaspour A, Takahashi M, Sairyo K *et al*. 2009; Optimal increase in bone mass by continuous local infusion of alendronate during distraction osteogenesis in rabbits. *Bone* **44**: 917–923.

Alge DL, Zhou D, Adams LL *et al*. 2010; Donor-matched comparison of dental pulp stem cells and bone marrow-derived mesenchymal stem cells in a rat model. *J Tissue Eng Regen Med* **4**: 73–81.

Alkaisi A, Ismail AR, Mutum SS *et al*. 2013; Transplantation of human dental pulp stem cells: enhance bone consolidation in mandibular distraction osteogenesis. *J Oral Maxillofac Surg* **71**1758: e1–13.

Al-Sharabi N, Xue Y, Fujio M *et al*. 2014; Bone marrow stromal cell paracrine factors direct osteo/odontogenic differentiation of dental pulp cells. *Tissue Eng A* **20**: 3063–3072.

Ando Y, Matsubara K, Ishikawa J *et al*. 2014; Stem cell-conditioned medium accelerates distraction osteogenesis through multiple regenerative mechanisms. *Bone* **61**: 82–90.

Aranha AM, Zhang Z, Neiva KG *et al*. 2010; Hypoxia enhances the angiogenic potential of human dental pulp cells. *J Endod* **36**: 1633–1637.

Ashton AW, Yokota R, John G *et al*. 1999; Inhibition of endothelial cell migration, intercellular communication, and vascular tube formation by thromboxane A(2). *J Biol Chem* **274**: 35562–35570.

Bikfalvi A, Klein S, Pintucci G *et al*. 1997; Biological roles of fibroblast growth factor-2. *Endocr Rev* **18**: 26–45.

Carano RA, Filvaroff EH. 2003; Angiogenesis and bone repair. *Drug Discov Today* **8**: 980–989.

Carmeliet P. 2003; Angiogenesis in health and disease. *Nat Med* **9**: 653–660.

Ceradini DJ, Kulkarni AR, Callaghan MJ *et al*. 2004; Progenitor cell trafficking is regulated by hypoxic gradients through HIF-1 induction of SDF-1. *Nat Med* **10**: 858–864.

Chen L, Tredget EE, Wu PY *et al*. 2008; Paracrine factors of mesenchymal stem cells recruit macrophages and endothelial lineage cells and enhance wound healing. *PLoS One* **3**: e1886.

Egusa H, Sonoyama W, Nishimura M *et al*. 2012; Stem cells in dentistry-part I: stem cell sources. *J Prosthodont Res* **56**: 151–165.

Enholm B, Paavonen K, Ristimäki A *et al*. 1997; Comparison of *VEGF*, *VEGF-B*, *VEGF-C* and *Ang-1* mRNA regulation by serum, growth factors, oncoproteins and hypoxia. *Oncogene* **14**: 2475–2483.

Fujio M, Yamamoto A, Ando Y *et al*. 2011; Stromal cell-derived factor-1 enhances distraction osteogenesis-mediated skeletal tissue regeneration through the recruitment of endothelial precursors. *Bone* **49**: 693–700.

Gong QM, Quan JJ, Jiang HW *et al*. 2010; Regulation of the stromal cell-derived factor-1α–CXCR4 axis in human dental pulp cells. *J Endod* **36**: 1499–1503.

Gronthos S, Mankani M, Brahim J *et al*. 2000; Postnatal human dental pulp stem cells (DPSCs) *in vitro* and *in vivo*. *Proc Natl Acad Sci USA* **97**: 13625–13630.

Halin C, Fahrngruber H, Meingassner JG *et al*. 2008; Inhibition of chronic and acute skin inflammation by treatment with a vascular endothelial growth factor receptor tyrosine kinase inhibitor. *Am J Pathol* **173**: 265–277.

Hung SC, Pochampally RR, Chen SC, *et al*. 2007; Angiogenic effects of human multipotent stromal cell conditioned medium activate the PI3K–Akt pathway in hypoxic endothelial cells to inhibit apoptosis, increase survival, and stimulate angiogenesis. *Stem Cells* **25**: 2363–2370.

Ide C, Nakai Y, Nakano N *et al*. 2010; Bone marrow stromal cell transplantation for treatment of sub-acute spinal cord injury in the rat. *Brain Res* **1332**: 32–47.

Ilizarov GA. 1989; The tension-stress effect on the genesis and growth of tissues: Part II. The influence of the rate and frequency of distraction. *Clin Orthop Relat Res* **239**: 263–285.

Inukai T, Katagiri W, Yoshimi R *et al*. 2013; Novel application of stem cell-derived factors for periodontal regeneration. *Biochem Biophys Res Commun* **430**: 763–768.

Isefuku S, Joyner CJ, Simpson AH. 2000; A murine model of distraction osteogenesis. *Bone* **27**: 661–665.

Kanczler JM, Oreffo RO. 2008; Osteogenesis and angiogenesis: the potential for engineering bone. *Eur Cell Mater* **15**: 100–114.

Kim HZ, Jung K, Kim HM *et al*. 2009; A designed angiopoietin-2 variant, pentameric COMP-Ang2, strongly activates Tie2 receptor and stimulates angiogenesis. *Biochim Biophys Acta* **1793**: 772–780.

Li G, Simpson AH, Kenwright J *et al*. 1999; Effect of lengthening rate on angiogenesis during distraction osteogenesis. *J Orthop Res* **17**: 362–367.

Lobov IB, Brooks PC, Lang RA. 2002; Angiopoietin-2 displays VEGF-dependent modulation of capillary structure and endothelial cell survival *in vivo*. *Proc Natl Acad Sci USA* **99**: 11205–11210.

Maisonpierre PC, Suri C, Jones PF *et al*. 1997; Angiopoietin-2, a natural antagonist for Tie2 that disrupts *in vivo* angiogenesis. *Science* **277**: 55–60.

Morishita R, Nakamura S, Hayashi S *et al*. 1999; Therapeutic angiogenesis induced by human recombinant hepatocyte growth factor in rabbit hind limb ischemia model as cytokine supplement therapy. *Hypertension* **33**: 1379–1384.

Osugi M, Katagiri W, Yoshimi R *et al*. 2012; Conditioned media from mesenchymal stem cells enhanced bone regeneration in rat calvarial bone defects. *Tissue Eng A* **18**: 1479–1489.

Park YS, Kim NH, Jo I. 2003; Hypoxia and vascular endothelial growth factor acutely upregulate angiopoietin-1 and *Tie2* mRNA in bovine retinal pericytes. *Microvasc Res* **65**: 125–131.

Pichiule P, Chavez JC, LaManna JC. 2004; Hypoxic regulation of angiopoietin-2 expression in endothelial cells. *J Biol Chem* **279**: 12171–12180.

Rubin J, Rubin C, Jacobs CR. 2006; Molecular pathways mediating mechanical signaling in bone. *Gene* **367**: 1–16.

Sakai K, Yamamoto A, Matsubara K *et al*. 2012; Human dental pulp-derived stem cells promote locomotor recovery after complete transection of the rat spinal cord by multiple neuro-regenerative mechanisms. *J Clin Invest* **122**: 80–90.

Shen K, Sheng Y, Ji L *et al*. 2010; Involvement of c-Jun *N*-terminal kinase and extracellular signal-regulated kinase 1/2 in EGF-induced angiogenesis. *Cell Biol Int* **34**: 1213–1218.

Shi S, Robey PG, Gronths S. 2001; Comparison of human dental pulp and bone marrow stromal stem cells by cDNA microarray analysis. *Bone* **29**: 532–539.

Stamatovic SM, Keep RF, Mostarica-Stojkovic M *et al*. 2006; CCL2 regulates angiogenesis via activation of Ets-1 transcription factor. *J Immunol* **177**: 2651–2661.

Suri C, Jones PF, Patan S *et al*. 1996; Requisite role of angiopoietin-1, a ligand for the TIE2 receptor, during embryonic angiogenesis. *Cell* **87**: 1171–80.
Toma C, Pittenger MF, Cahill KS *et al*. 2002; Human mesenchymal stem cells differentiate to a cardiomyocyte phenotype in the adult murine heart. *Circulation* **105**: 93–98.
Wang JH, Thampatty BP. 2006; An introductory review of cell mechanobiology. *Biomech Model Mechanobiol* **5**: 1–16.
Wang Y, Wan C, Deng L *et al*. 2007; The hypoxia-inducible factor-α pathway couples angiogenesis to osteogenesis during skeletal development. *J Clin Invest* **117**: 1616–1626.
Watson JT. 2006; Distraction osteogenesis. *J Am Acad Orthop Surg* **14**: S168–174.
Yamada Y, Ueda M, Naiki T *et al*. 2004; Autogenous injectable bone for regeneration with mesenchymal stem cells and platelet-rich plasma: tissue-engineered bone regeneration. *Tissue Eng* **10**: 955–964.

Supporting information on the internet

The following supporting information may be found in the online version of this article:

Figure S1. (A) Schematic drawing of the branch points, tube length and tube formation area defined in this study: white, branch point; blue, tube length; yellow, tube formation area. (B) The distraction zone was defined as the area enclosed in a quadrangle, with its four end points being the osteotomized lines. The cartilage-/bone-formation areas were calculated using the equation:

Newly formed cartilage area (%) = (new cartilage area/distraction zone) × 100

DOI: 10.1002/term